

Charmed-meson spectroscopy in QCD sum rule

A. Hayashigaki¹ and K. Terasaki²

¹ *Department of Physics, Kyoto University, Kyoto 606-8502, Japan** and

² *Yukawa Institute for Theoretical Physics, Kyoto University, Kyoto 606-8502, Japan[†]*

(Dated: August 7, 2021)

We elaborate masses of open-charm mesons ($c\bar{d}$ and $c\bar{s}$) with $J^P = 0^-, 1^-, 0^+, 1^+$ from a viewpoint of ordinary light-heavy systems in the analysis of standard Borel-transformed QCD sum rule. This analysis is implemented with the operator product expansion up to dimension 6, permitting corrections to the order α_s and to the order m_s , and without relying on $1/m_c$ -expansion. The obtained results following our stringent criteria for the continuum-threshold dependence, the Borel window and the Borel stability, indicate that the charmed-meson masses in the 0^+ channel are overestimated by $100 \sim 200$ MeV in comparison with the experimental data, which were recently reported as the rather broad state of $D^{*+}(2351)$ and the extremely narrow state of $D_s^{*+}(2317)$, respectively. Such large mass-discrepancies from the data cannot be seen in other channels, where conversely our results of the $c\bar{s}$ -meson masses are even underestimated somewhat in comparison with data, independent of the value of the strange-quark mass adopted in our calculations. From these results, it might be expected that the measured low mass of $D_s^{*+}(2317)$ is a manifestation of an exotic state with the structures of a four-quark or a molecule, while at present the D^{*+} is not in conflict with the existing data due to its large width.

PACS numbers: 14.40.Lb, 12.38.-t, 11.55.Hx, 11.55.Fv

I. INTRODUCTION

The detailed study of charmed-meson spectroscopy has provided us with understanding of not only its structure and property peculiar to the light-heavy system, but also widely the basic property of the strong interactions. Especially, the charmed mesons have played a part for the success of a potential model analysis in meson spectroscopy through a unified framework [1]. However, recent experimental discovery of scalar and axial-vector $c\bar{s}$ -mesons [2, 3, 4, 5, 6], which have been only missing p -wave states [7], cast a shadow on such a success of the potential models, because their predictions [8, 9, 10] give heavier masses by $100 \sim 200$ MeV than the observations. Similar results have been seen also in QCD sum rule coupled with heavy quark effective theory (HQET) [11] and lattice QCD simulations [12, 13]. In the meanwhile, an interpretation of states with $J^P = 0^+, 1^+$ as the chiral partner of ground states with $0^-, 1^-$ in the heavy quark limit requires relatively lower masses for the $(0^+, 1^+)$ states than the above predictions. The analysis based on such idea gives the results comparable to the observations [14, 15]. This problem with the mass discrepancy has triggered a lot of debates on the natures of the $c\bar{s}$ mesons in the viewpoints of modification of theoretical models, *e.g.* involving DK -mixing [16], or introduction of unconventional structures like two-meson molecular states [17, 18] or four-quark states [19, 20] or

their mixture [21]. There is, however, still no definite explanation for the discrepancy.

In this paper, we study eight states of the charmed mesons with $J^P = 0^-, 1^-, 0^+, 1^+$, which are composed of the corresponding four states of $c\bar{s}$ -mesons and similarly four states of $c\bar{n}$ -mesons with $n = u, d$. The masses of their states are elaborated through all the same analysis from the viewpoint of the conventional interpretation as light-heavy-quark bound systems. We then focus attention on the masses of two $c\bar{s}$ -mesons with 0^+ and 1^+ in comparison with the experimental data. This method would be quite useful to extract information on specific states like 0^+ and 1^+ in the analysis involving relatively large theoretical uncertainties. Here, in the 1^+ channel, we deal with only a channel of charge-conjugation parity $+1$, *i.e.* $J^{P(C)} = 1^{+(+)}$ channel, although indeed the light-heavy system does not have this parity as a good quantum number and thus takes place a mixing between $1^{+(+)}$ and $1^{+(-)}$ channels.

In the present work, such a physical motivation can be realized technically by relying on the standard QCD sum rule (QSR) approach [22, 23], which evaluates hadron properties by using the correlator of the quark currents over the physical vacuum. We perform its calculation without taking $1/m_c$ -expansion, where m_c is the charm quark mass. It is because the charm quark is comparatively light and some properties of charmed-meson systems seem to be not necessarily valid for such an expansion, especially for their masses. However, some analyses have approximated at the first few terms of the expansion based on the HQET [9, 10, 11, 12]. Our analysis is implemented with the operator product expansion up to dimension 6, permitting corrections to the order α_s and

*Electronic address: arata@ruby.scphys.kyoto-u.ac.jp

[†]Electronic address: terasaki@yukawa.kyoto-u.ac.jp

to the order m_s , where α_s is strong coupling constant and m_s the strange-quark mass. In Borel-transformed QSR, so-called Borel sum rule (BSR) [22], we extract charmed-meson masses with imposing criteria for the continuum-threshold dependence, the Borel window and the Borel stability. Indeed, we find that the $D(0^+)$, $D_s(0^+)$ -meson masses are overestimated by $100 \sim 200$ MeV compared with the experimental data, while such a tendency cannot be seen in other channels. Conversely, in other channels the $c\bar{s}$ -meson masses are even underestimated somewhat in comparison with the data, independent of the value of the strange-quark mass adopted in our analysis. Accounting for the measured broad width of the $D(0^+)$ -meson, the state seems to be not in conflict with the existing data. From these results, it is quite possible that the measured low mass of $D_s^{*+}(2317)$ is a manifestation of any exotic states with the structures of a four-quark or a molecule.

This paper is organized as follows. In sec. II, we first mention the current status of charmed-meson spectroscopy in more detail, from both experimental and theoretical aspects. In sec. III, we formulate the general form of BSR and derive the analytic forms of $c\bar{s}$ -mesons in four channels of $0^-, 1^-, 0^+, 1^+$, respectively, and similar relations for the $c\bar{n}$ mesons are also easily obtained. Our criteria requested in the analysis of BSR are given in sec. IV and numerical results obtained thus are also shown. Finally, summary and discussion are devoted in sec. V.

II. CHARMED-MESON SPECTROSCOPY

In general, the classification of mesons containing a single heavy quark is interpreted with the help of heavy-quark symmetry (HQS) [7], *i.e.* the symmetry valid for the infinitely heavy mass of charm quark. Under this symmetry, the strong interaction conserves total angular momentum of the light quark, j . In the meanwhile, total angular momentum of the light-heavy system, J , should be still regarded as a good quantum number of the system, even if the HQS breaks down. Indeed, the charm quark is much heavier than the QCD scale ($\Lambda_{\text{QCD}} \simeq 0.25$ GeV) but not infinitely heavy. In this way, we explain the classification of charmed mesons in terms of (L, S, J, j) appropriately according to circumstances. Here L and S denote the orbital angular momentum between the light and heavy quarks and total spin of the system, respectively. For instance, two ground states ($L = 0, J^{P(C)} = 0^{-(+)}, 1^{(-)}$) form the $j = 1/2$ doublets and four the first excited states ($L = 1, J^{P(C)} = 0^{+(+)}, 1^{+(+)}, 1^{+(-)}, 2^{+(+)}$) can be understood as $j = 1/2$ doublets ($J^{P(C)} = 0^{+(+)}, 1^{+(+)}$) and $j = 3/2$ doublets ($J^{P(C)} = 1^{+(-)}, 2^{+(+)}$). The states up to $L = 1$ with two classifications are shown in the horizontal axis of Fig. 1.

Four of these six states, *i.e.* $j = 1/2$ doublets at $L = 0$ and $j = 3/2$ doublets at $L = 1$, have been observed

over the past two decades ($\sim 1975 - 1994$) following the discovery of open charms [7], because their states have relatively narrow widths [24]. The properties of masses and widths for both charmed non-strange and strange mesons match well with the predictions from the potential model analyses [1, 8, 9]. Recently (2000 \sim), the leading candidates for two missing states, $j = 1/2$ doublets at $L = 1$, have been also discovered: the first observation of D_1^0 with the features of $J^P = 1^+$ was reported by the CLEO Collaboration [25] and it was also observed by the BELLE Collaboration [26]. The D_1^0 has the mass $M_{D_1^0} \simeq 2423$ MeV and the very broad width $\Gamma_{D_1^0} \simeq 329$ MeV, where we adopted the average of the above two data. Besides the D_1^0 , the BELLE Collaboration observed also a very broad resonance D_0^{*0} with the features of $J^P = 0^+$ [26]. Though a marginally compatible result with that of the BELLE for the mass, the FOCUS Collaboration also confirmed the evidence of the D_0^{*0} and at the same time observed its charged partner D_0^{*+} , which also has the rather broad width [27]. The average of the BELLE and FOCUS data on the D_0^{*0} gives $M_{D_0^{*0}} \simeq 2351$ MeV and $\Gamma_{D_0^{*0}} \simeq 262$ MeV. The FOCUS data on the D_0^{*+} is $M_{D_0^{*+}} \simeq 2403$ MeV and $\Gamma_{D_0^{*+}} \simeq 283$ MeV. As seen from these data, the $j = 1/2$ doublets at $L = 1$ have the very broad widths of several hundreds MeV in contrast with the $j = 3/2$ doublets at $L = 1$. Their masses and broad widths are not in conflict with predictions from the potential model analyses [8, 9]. Very recently, also for the charmed-strange mesons four experimental groups (BABAR, CLEO, BELLE, FOCUS) independently have observed the leading candidates for missing $j = 1/2$ doublets at $L = 1$. Contrary to our natural speculation about their masses and widths in analogy with the charmed non-strange mesons, surprising facts were reported by the observations of their groups, as mentioned below in detail.

The $D_{s_0}^{*+}(2317)$ was first discovered in the $D_s^+\pi^0$ decay channel with the very narrow width by the BABAR Collaboration [2], and in the same decay channel its existence was soon later confirmed by the CLEO [4] and the BELLE [5] Collaborations. Its mass was measured to be 2317 MeV commonly, which is approximately 46 MeV below the DK threshold. The width was determined to be less than 4.6 MeV, which is compatible with the experimental resolution. Here we adopted the severest upper bound from the BELLE [5]. More recently, the FOCUS Collaboration [6] reported a preliminary result on the measurement of the mass 2323 MeV, slightly larger than those from the other three experiments. Together with the $D_{s_0}^{*+}(2317)$, the CLEO [4] and the BELLE [5] observed another narrow resonance in the $D_s^+\pi^0$ decay channel, with the mass close to 2.46 GeV, where we denote the state by $D_{s_1}^+$. Later, the BABAR confirmed its existence in the same decay channel [3], although they have already found such a signal in Ref. [2]. It can be assigned to $J^P = 1^+$ from the observation of the radiative decay in $D_s^+\gamma$ and the analysis of helicity distributions.

Their average mass is 2459 MeV, which is approximately 46 MeV below $D^{*+}K^0$ and the width is less than 5.5 MeV, which is the severest upper bound observed by the BELLE [5].

On the other hand, prior to such observations, most potential models as typified by Refs. [8, 9] have predicted that two missing states of 0^+ and 1^+ ($L = 1, j = 1/2$ doublets) should be massive enough to decay into DK and D^*K in a s -wave, respectively. The widths are then expected to be very broad due to the strong decays. The spectroscopy of $c\bar{n}$ and $c\bar{s}$ mesons with $L = 0, 1$ is drawn in Fig. 1 in order to compare theoretical predictions (solid lines for the $c\bar{s}$ and dashed lines for the $c\bar{n}$) with the experimental data (closed circle for the $c\bar{s}$ and open circle for the $c\bar{n}$). We refer to numerical results in Ref. [8] as a typical calculation by the potential models. Their values on the masses are written down in the figure. After

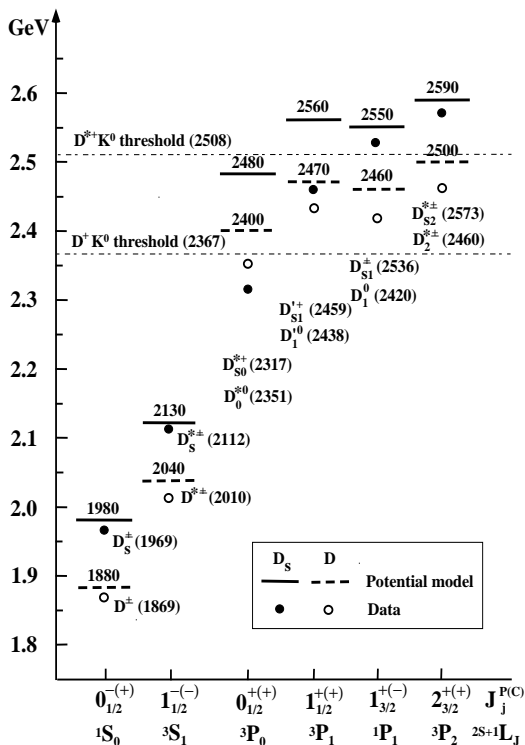


FIG. 1: Spectroscopy of $c\bar{n}$ and $c\bar{s}$ mesons with $L = 0, 1$. The solid lines for the $c\bar{s}$ and dashed lines for the $c\bar{n}$ show numerical results quoted from Ref. [8] and the experimental data to be compared are given by closed and open circles [2, 3, 4, 5, 6, 24, 25, 26, 27], respectively. Their values on the masses are written down in this figure. For the purpose of reference, two dash-dotted lines display the thresholds of D^+K^0 and $D^{*+}K^0$ decays for the $c\bar{s}$ mesons.

the observations, using data of their new states, Cahn and Jackson [10] showed that there are no model parameters to explain all the masses and widths of the 0^+ and 1^+ states consistently within the potential models. Thus, large discrepancies between the observations and the theoretical predictions for the masses and the widths have

renewed theoretical interests in the issue of the charmed-strange meson spectroscopy, especially for the 0^+ state [28]. Such a large discrepancy of the mass in the 0^+ channel is seen also in the QCD sum rule analysis based on HQET [11] and lattice QCD calculations in the static limit [12] or with dynamical quarks [13], although their analyses still have large errors. To resolve this issue, a lot of theoretical ideas have been suggested. These ideas would be categorized broadly into two cases: modification of prior conventional models or claim of exotic states different from prior conventional structures. As one of improvements within the context of conventional quark models, it was shown that the DK mixing with the p -wave $c\bar{s}$ state plays an important role to lower the mass [16]. Apart from such a conventional picture, a possibility of the exotic configuration has been suggested: a four-quark state [19, 20, 29], DK molecule [17], $D_s\pi$ atom [18], and four-quark states with a DK mixing [21]. Using perturbative QCD, Chen and Li calculated branching ratios of D_{s0}^{*+} (2317) productions in the B -meson decays and showed that the BELLE measurement of B -meson decays favors exotic multi-quark states of the D_{s0}^{*+} (2317), rather than conventional pictures [30]. However, it was argued that four-quark states could not be bound for the charmed-strange mesons [31]. Thus, the theoretical verdict on this crucial issue is still not obtained.

Another remarkable property of light-heavy systems is that in the heavy quark limit the $j = 1/2$ doublets at $L = 1$ could be interpreted as a chiral partner of those at $L = 0$ [14, 15]. According to this idea, one could expect that the mass-splittings between the $0^+(1^+)$ and $0^-(1^-)$ states are almost equivalent to $m_N/3$, where m_N is a nucleon mass. The masses of the 0^+ and 1^+ states obtained from this value are indeed near the values measured by experiments. This property requires us comprehensive discussion involving not only the excited states of 0^+ and 1^+ but also the ground states of 0^- and 1^- , when we investigate the masses of 0^+ and 1^+ states in detail.

Motivated by these, we formulate the QSRs and show the Borel-transformed forms for eight states of the $c\bar{s}$ and $c\bar{n}$ mesons with $J^{PC} = 0^-, 1^-, 0^+, 1^+$ in the next section. Note that we study these eight states independently in all the same framework and criteria for the BSR, and discuss their relative energy levels.

III. FORMULATION OF BOREL SUM RULES

We start by considering the covariant two-point function $\Pi_R(q^2)$ with quark currents $J_R(x)$ ($R = 0^-, 1^-, 0^+, 1^+$) [22, 32]

$$\Pi_R(q^2) = i \int d^4x e^{iq \cdot x} \langle 0 | T J_R(x) J_R^\dagger(0) | 0 \rangle, \quad (1)$$

where $|0\rangle$ is nonperturbative QCD vacuum and T the time-ordered product. $J_R(x)$ denotes the pseudo-scalar,

vector, scalar and axial-vector currents described respectively as

$$J_{0-}(x) = i\bar{q}(x)\gamma_5 c(x), \quad (2)$$

$$J_{1-}^\mu(x) = \bar{q}(x)\gamma^\mu c(x), \quad (3)$$

$$J_{0+}(x) = \bar{q}(x)c(x), \quad (4)$$

$$J_{1+}^\mu(x) = \eta^{\mu\nu}\bar{q}(x)\gamma_\nu\gamma_5 c(x), \quad (5)$$

with $q(x)$ being light-quark (d or u under the isospin symmetry) fields or strange-quark (s) field and $c(x)$ being charm-quark field at the point x , and $\eta^{\mu\nu} = q^\mu q^\nu / q^2 - g^{\mu\nu}$. Note that, e.g., the Lorentz structure of the vector-current correlator with $J_{1-}^\mu(x)$ and $J_{1-}^{\nu\dagger}(0)$ can be generally expressed as the sum of the transverse invariant function proportional to $q^\mu q^\nu / q^2 - g^{\mu\nu}$ and the longitudinal invariant function proportional to $q^\mu q^\nu / q^2$. We here confine our attention to only the transverse component. In the axial-vector case, automatically only the transverse component remains owing to addition of Lorentz tensor $\eta^{\mu\nu}$ and hence we can get rid of the contribution from the pseudo-scalar meson in the lowest state [33].

We define invariant functions $\Pi_i(q^2)$ ($i = P, V, S, A$), which are directly evaluated in our QSR, for respective channels as follows: $\Pi_{0-}(q^2) = \Pi_P(q^2)$, $\Pi_{1-}^{\mu\nu}(q^2) = (q^\mu q^\nu / q^2 - g^{\mu\nu})\Pi_V(q^2)$, $\Pi_{0+}(q^2) = \Pi_S(q^2)$ and $\Pi_{1+}^{\mu\nu}(q^2) = (q^\mu q^\nu / q^2 - g^{\mu\nu})\Pi_A(q^2)$. Under these definitions, the dispersion relation satisfied by such invariant functions is given without any subtraction as

$$\Pi(q^2) = \frac{1}{\pi} \int ds \frac{\text{Im}\Pi(s)}{s - q^2 - i\epsilon}. \quad (6)$$

This equation relates the real part of the correlation function, which is valid in the high momentum region ($-q^2 \rightarrow \infty$), with the imaginary part, which is valid in the low momentum region ($q^2 \rightarrow \Lambda_{QCD}^2$) with a typical soft-scale Λ_{QCD} . Via this dispersion relation, we construct the QSR by equating the side of operator product expansion (OPE) and the phenomenological (PH) side related to the spectral function. The former is described as the product of Wilson coefficients and nonperturbative QCD vacuum condensates or quark masses, while the latter is parametrized by hadronic quantities such as resonance masses, couplings and the continuum threshold, *etc.* Thus, the QSR is represented in a simple form,

$$\int_{m_c^2}^{\infty} ds W(s) \frac{1}{\pi} (\text{Im}\Pi^{PH}(s) - \text{Im}\Pi^{OPE}(s)) = 0, \quad (7)$$

where $W(s)$ is an arbitrary weight function, but must be analytic except for the positive real axis. The lower limit of the integration is given by the charm-quark Mass squared, m_c^2 . We adopt $W(s) = \exp(-s/M^2)$ in the BSR below, where M is known as an artificial so-called Borel mass. We take the most general ansatz for the spectral function of the PH side, *i.e.*, it would be saturated by one resonance in the narrow width limit and a continuum in

the form of a step function:

$$\begin{aligned} & \frac{1}{\pi} \text{Im}\Pi^{PH}(s) \\ &= F\delta(s - m_R^2) + \frac{1}{\pi} \text{Im}\Pi^{OPE}(s)\theta(s - s_R) \end{aligned} \quad (8)$$

with the QCD continuum threshold s_R . F is a pole residue, where we take $F = f_R^2 m_R^{2k}$ with f_R the couplings of the lowest resonances with respective parities to the hadronic current and m_R a pole mass. The power k of m_R^2 in the pole residue is taken to match the maximum power of s in the asymptotic s -behavior of the spectral function. For $s > s_R$, we assume that the hadronic continuum reduces to the same form with that obtained by an analytic continuation of the OPE, *i.e.* the perturbative terms, based on a hypothesis of the quark-hadron duality. Such an assumption is expected to smear the contributions of the higher radial excitations. This simple ansatz would indeed reproduce well the characteristic features of the real spectrum in most applications of sum rules to mesons and baryons [32].

Next, we display analytic forms of the QSR in each channel by implementing the Borel transformation to the QSR as in Eq. (7) [34]. Performing the OPE at dimension $d \leq 6$ operators, we obtain the relations of the BSR for four channels ($0^+, 0^-, 1^+, 1^-$) of the $c\bar{s}$ meson: in the scalar 0^+ (pseudoscalar 0^-) channels, those read

$$\begin{aligned} & f_{0^\pm}^2 m_{0^\pm}^2 e^{-m_{0^\pm}^2/M^2} \\ &= \frac{3}{8\pi^2} \int_{m_c^2}^{s_{0^\pm}} ds e^{-s/M^2} s \left(1 - \frac{m_c^2}{s}\right)^2 \\ &\times \left(1 \mp \frac{2m_c m_s}{s - m_c^2} + \frac{4}{3} \frac{\alpha_s(s)}{\pi} R_0(m_c^2/s)\right) \\ &+ e^{-m_c^2/M^2} \left[\pm m_c \langle \bar{s}s \rangle_0 + \frac{1}{2} \left(1 + \frac{m_c^2}{M^2}\right) m_s \langle \bar{s}s \rangle_0\right. \\ &+ \frac{1}{12} \left(\frac{3}{2} - \frac{m_c^2}{M^2}\right) \left\langle \frac{\alpha_s}{\pi} G^2 \right\rangle_0 \\ &\pm \frac{1}{2} \frac{1}{M^2} \left(1 - \frac{1}{2} \frac{m_c^2}{M^2}\right) m_c \langle \bar{s}g\sigma \cdot Gs \rangle_0 \\ &- \frac{1}{12} \frac{m_c^4}{M^6} m_s \langle \bar{s}g\sigma \cdot Gs \rangle_0 \\ &\left. - \frac{16\pi}{27} \frac{1}{M^2} \left(1 + \frac{1}{2} \frac{m_c^2}{M^2} - \frac{1}{12} \frac{m_c^4}{M^4}\right) \alpha_s \langle \bar{s}s \rangle_0^2\right], \end{aligned} \quad (9)$$

where g denotes the strong coupling, $G^2 = G_{\mu\nu}G^{\mu\nu}$ with gluon field $G_{\mu\nu}$ and $\sigma \cdot G = \sigma_{\mu\nu}G^{\mu\nu}$. $\langle O \rangle_0$ with the composite operator O represents $\langle 0|O(0)|0 \rangle$ with the local composite operator $O(0)$ at the origin. On the other hand, in the axial-vector 1^+ (vector 1^-) channels, we

similarly obtain

$$\begin{aligned}
& f_{1\pm}^2 m_{1\pm}^2 e^{-m_{1\pm}^2/M^2} \\
&= \frac{1}{8\pi^2} \int_{m_c^2}^{s_{1\pm}} ds e^{-s/M^2} s \left(1 - \frac{m_c^2}{s}\right)^2 \left(2 + \frac{m_c^2}{s}\right) \\
&\times \left(1 \mp \frac{3m_c m_s s}{(2s + m_c^2)(s - m_c^2)} + \frac{4}{3} \frac{\alpha_s(s)}{\pi} R_1(m_c^2/s)\right) \\
&+ e^{-m_c^2/M^2} \left[\pm m_c \langle \bar{s}s \rangle_0 + \frac{1}{2} \frac{m_c^2}{M^2} m_s \langle \bar{s}s \rangle_0 \right. \\
&- \frac{1}{12} \left\langle \frac{\alpha_s}{\pi} G^2 \right\rangle_0 \mp \frac{1}{4} \frac{m_c^2}{M^4} m_c \langle \bar{s}g\sigma \cdot Gs \rangle_0 \\
&+ \frac{1}{12} \frac{1}{M^2} \left(1 + \frac{m_c^2}{M^2} - \frac{m_c^4}{M^4}\right) m_s \langle \bar{s}g\sigma \cdot Gs \rangle_0 \\
&\left. - \frac{20\pi}{81} \frac{1}{M^2} \left(1 + \frac{m_c^2}{M^2} - \frac{1}{5} \frac{m_c^4}{M^4}\right) \alpha_s \langle \bar{s}s \rangle_0^2 \right]. \quad (10)
\end{aligned}$$

Here, we approximate at the first order of m_s , because m_s is small enough compared to m_c or a typical scale of M ($M \sim 1$ GeV). The $O(\alpha_s)$ corrections to the perturbative contributions are given as the function $R_0(x)$ for the (pseudo-) scalar channel [35, 36] and the function $R_1(x)$ for the (axial-) vector channel [36, 37] as follows:

$$\begin{aligned}
R_0(x) &= \frac{9}{4} + 2Li_2(x) + \ln x \ln(1-x) - \frac{3}{2} \ln \frac{1-x}{x} \\
&- \ln(1-x) + x \ln \frac{1-x}{x} - \frac{x}{1-x} \ln x \quad (11)
\end{aligned}$$

$$\begin{aligned}
R_1(x) &= \frac{13}{4} + 2Li_2(x) + \ln x \ln(1-x) - \frac{3}{2} \ln \frac{1-x}{x} \\
&- \ln(1-x) + x \ln \frac{1-x}{x} - \frac{x}{1-x} \ln x \\
&+ \frac{(3+x)(1-x)}{2+x} \ln \frac{1-x}{x} - \frac{2x}{(2+x)(1-x)^2} \ln x \\
&- \frac{5}{2+x} - \frac{2x}{2+x} - \frac{2x}{(2+x)(1-x)} \quad (12)
\end{aligned}$$

with the Spence function $Li_2(x) = -\int_0^x dt t^{-1} \ln(1-t)$. As for the running coupling constant $\alpha_s(s)$ appearing in the perturbative terms of Eqs. (9) and (10), we approximate it by a one-loop form, $\alpha_s(s) = 4\pi/(9\ln(s/\Lambda_{QCD}^2))$ with $\Lambda_{QCD}^2 = (0.25 \text{ GeV})^2$, which is determined to reproduce $\alpha_s(1 \text{ GeV}) \simeq 0.5$ [38].

As easily seen from Eqs. (9) and (10), we can get the relations of the OPE in the 0^- and 1^- channels by replacing simply m_c by $-m_c$ for those in the 0^+ and 1^+ . Also, replacing m_s and $\bar{s}s$ by m_n and $\bar{n}n$ respectively, we can derive the corresponding BSRs for the non-strange $c\bar{n}$ mesons except for the only difference of the continuum thresholds. We here take the massless limit ($m_n = 0$) of light quarks for the BSR of the $c\bar{n}$ mesons. These results indeed reproduce the corresponding BSRs for light mesons in the vector, scalar and axial-vector channels (see the results of Ref. [39] in vacuum). Looking on the relations of OPE in the right-hand sides of (9) and (10), we find that the difference of property between the $c\bar{n}$

and $c\bar{s}$ mesons would be caused by the effect of strange quarks that is mainly the difference between lowest dimensional condensates, $m_c \langle \bar{n}n \rangle_0$ and $m_c \langle \bar{s}s \rangle_0$. For the pseudoscalar channel of the $c\bar{n}$ mesons, the similar relation was used in Ref. [40], although their relations are somewhat different from ours for whole sign of a term including gluon condensate and a part of terms including four-quark condensates. This difference, however, is insensitive to the final results. For the axial and vector channels of the $c\bar{n}$ mesons, under approximation neglecting gluon condensates and four-quark condensates, the same relation was used in Ref. [41]. More recently, Narison presented explicit BSR forms in the scalar and pseudoscalar channels of the $c\bar{n}$ and $c\bar{s}$ mesons [23]. They are very similar to our forms.

In order to extract the values of physical quantities from the BSR, we use the following standard values for QCD parameters appearing in the OPE: $m_s = 0.12$ GeV [32], $m_c = 1.46$ GeV [42], $\langle \bar{n}n \rangle_0 = (-0.225 \text{ GeV})^3$ [32], $\langle \bar{s}s \rangle_0 = 0.8 \times \langle \bar{n}n \rangle_0 \text{ GeV}^3$ [32], $\langle \frac{\alpha_s}{\pi} G^2 \rangle_0 = (0.33 \text{ GeV})^4 \times 2$ [36], $\langle \bar{n}g\sigma \cdot Gn \rangle_0 = M_0^2 \langle \bar{n}n \rangle_0$ with $M_0^2 = 0.8 \text{ GeV}^2$ [43], $\langle \bar{s}g\sigma \cdot Gs \rangle_0 = M_0^2 \langle \bar{s}s \rangle_0$, $\alpha_s \langle \bar{n}n \rangle_0^2 = 0.162 \times 10^{-3} \text{ GeV}^6$ and $\alpha_s \langle \bar{s}s \rangle_0^2 = 0.8^2 \times \alpha_s \langle \bar{n}n \rangle_0^2 \text{ GeV}^6$. Note that we evaluated four-quark condensates in terms of $\langle \bar{n}n \rangle_0$, supposing that the factorization or vacuum saturation in an intermediate state of four-quark matrix element can work well in a good approximation [22]. Although the ambiguity of the absolute value of the four-quark condensate still remains large as discussed by several authors (see Refs. [36, 43]), the detailed discussion is not much relevant to our present analysis. It is because the contribution from higher dimensional condensates is negligible compared to the lowest dimensional operators ($d = 3$) and thus the final results are independent of details of four-quark condensates.

Finally, taking a logarithmic derivative with respect to $1/M^2$ for both sides of (9) and (10), we get rid of f_R^2 -dependence completely from their equations and thus can derive the Borel curve of the resonance masses m_R^2 as functions of M^2 and s_R .

IV. NUMERICAL RESULTS

We determine plausible values of the resonance mass extracted from the Borel curves in accordance with the following criteria. Its method is in order:

1. We plot the Borel curves of the resonance mass m_R as a function of M with taking some selected values of the continuum thresholds $\sqrt{s_R}$. In general, the values of the thresholds might be different from the phenomenological value of the first radial excitation mass and rather would be smaller. This is natural, because our simple ansatz in the PH side of the QSR cannot take into account the complicated structure of the resonances in this region. We, therefore, set the maximum value of $\sqrt{s_R}$, $\sqrt{s_R^{max}}$,

to be the mass of the first radial excitation predicted by the potential model [9].

2. In the OPE side, the contribution of the nonperturbative corrections should be generally small compared to that of the perturbative terms in large momentum region. Since we, however, truncate the OPE at $d = 6$ by hand, we would make the impact of this approximation as small as possible. In naive sense it is satisfied requiring that the contribution from higher dimensional operators than $d = 6$ becomes thoroughly smaller than the perturbative terms in large region of M . In such a region of M , the convergence of the OPE can indeed be ensured to some extent. Here, we quantitatively require a constraint that the effect of $d = 6$ term is less than 20% compared to that of the leading terms in Eqs. (9) and (10). This assures us to get physical quantities with about 10 ~ 20% accuracy. This condition gives the lower limit of M , M_{min} .
3. In the PH side, we would make the continuum contribution as small as possible, since we are interested only in the pole mass. It would be possible by taking small region of M . We require that the continuum contribution is less than 20% compared to that of the perturbative contribution. For the leading terms in Eqs. (9) and (10), the continuum contribution corresponds to the integration over s from s_R to infinity, while the perturbative contribution has the integration from m_c^2 to infinity. This constraint also assures us to get physical quantities with about 10 ~ 20% accuracy. From this condition, we can give the upper limit of M , M_{max} , which strongly depends on the threshold in contrast to M_{min} .
4. Thus, we set the Borel window, $M_{min} < M < M_{max}$, so that the BSR would work well within the window and we extract more reliable values of physical quantities from the Borel curves.
5. For $\sqrt{s_R} < \sqrt{s_R^{max}}$, we look for the stable regions (Borel stability) of the Borel curves vs. M within the Borel windows. Then, from the curve having the widest Borel stability, we read off the resonance mass and the threshold as the most reliable values of physical quantities. In general, this would give the central values of physical quantities under consideration. Finally, we adopt all resonance masses and thresholds to the extent that the Borel stabilities on the curves exist within the Borel windows. This would give errors for the central values. Note that in actual evaluation for the Borel stability we do not mind its accurate positions and widths of the stable regions. Such an ambiguity also should be included in the above errors.

Following the above criteria, we plot the Borel curves of resonance masses m_R vs. M in two ground states

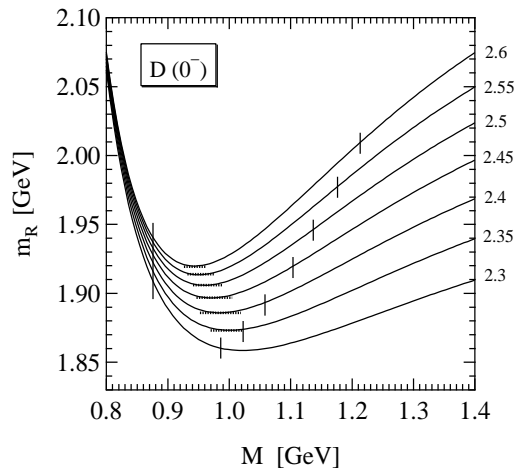


FIG. 2: The Borel curves of $m_{D(0^-)}$ vs. M , where $\sqrt{s_{D(0^-)}} = 2.3 \sim 2.6$ GeV at 0.05 GeV intervals. Explanation for the lines is given in the text.

($R = 0^-, 1^-$) of the $c\bar{n}$ mesons. We first study these two channels to determine a size of charm-quark mass m_c , which is treated as an input data in the OPE side. Since the quark mass is a scale-dependent quantity, its size runs with the energy scale of the system, *e.g.* we adopt $m_c = 1.2 \sim 1.5$ GeV in the QSR approach [44, 45]. We determine m_c to reproduce the masses of both states as well as possible. This leads to $m_c = 1.46$ GeV as listed before. Using this input, we shows the curves for the 0^-

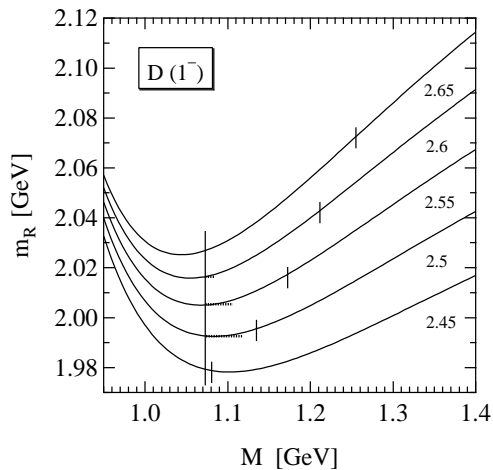


FIG. 3: The Borel curves of $m_{D(1^-)}$ vs. M , where $\sqrt{s_{D(1^-)}} = 2.45 \sim 2.65$ GeV at 0.05 GeV intervals.

channel with $\sqrt{s_{D(0^-)}} = 2.3 \sim 2.6$ GeV at 0.05 GeV intervals in Fig. 2 and for the 1^- channel with $\sqrt{s_{D(1^-)}} = 2.45 \sim 2.65$ GeV at 0.05 GeV intervals in Fig. 3. In Fig. 2, left long (right short) vertical-lines on the curves represents the lower (upper) limit of the Borel window, $M_{min}(M_{max})$, which very weakly decreases (strongly increases) with the threshold. We show the Borel stabilities

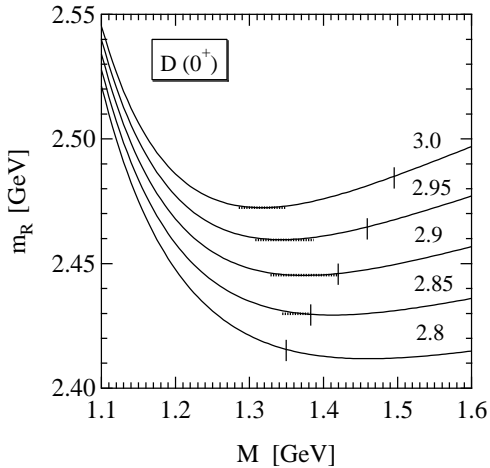


FIG. 4: The Borel curves of $m_{D(0^+)}$ vs. M , where $\sqrt{s_{D(0^+)}} = 2.8 \sim 3.0$ GeV at 0.05 GeV intervals. The lower limits of the Borel windows are below $M = 1.1$ GeV.

by dotted lines within these Borel windows. The length of the lines corresponds to the range of stable regions. In

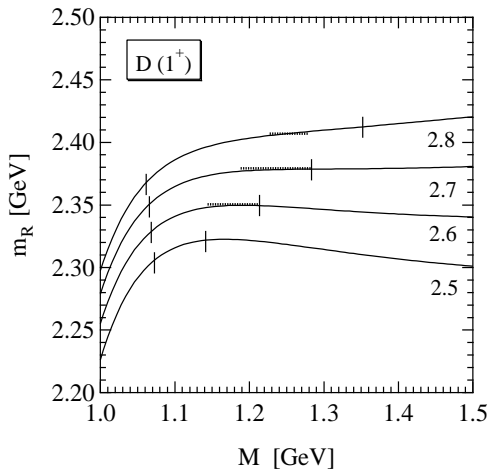


FIG. 5: The Borel curves of $m_{D(1^+)}$ vs. M , where $\sqrt{s_{D(1^+)}} = 2.5 \sim 2.8$ GeV at 0.1 GeV intervals.

the 0^- channel, we cannot find any Borel stability below $\sqrt{s_{D(0^-)}} = 2.3$ GeV, while above the value there exist such stable regions on the curves until the upper limit $\sqrt{s_{D(0^-)}} = 2.6$ GeV. Thus, we get the resonance mass, $m_{D(0^-)} = 1.90 \pm 0.03$ GeV. In the 1^- channel, we cannot find any Borel stability below $\sqrt{s_{D(1^-)}} = 2.45$ GeV, while above the value there exist such stable regions on the curves until $\sqrt{s_{D(1^-)}} = 2.6$ GeV, which is below the upper limit $\sqrt{s_{D(1^-)}} = 2.7$ GeV. Thus, we get the resonance mass, $m_{D(1^-)} = 2.00 \pm 0.02$ GeV. Indeed, the obtained results for resonance masses are near experimental values, $m_{D(0^-)}^{exp.} \simeq 1.867$ GeV and $m_{D(1^-)}^{exp.} \simeq 2.010$ GeV, respectively. In a similar analysis, we get the results of other channels, $m_{D(0^+)} = 2.45 \pm 0.03$ GeV and

TABLE I: Numerical results of the resonance mass m_R and the continuum threshold $\sqrt{s_R}$. They are listed for four channels ($R = 0^-, 1^-, 0^+, 1^+$) of the $c\bar{c}$ mesons. We refer to Ref. [24, 26] for the experimental data and the predictions from Ref. [9] for maximum values of the thresholds.

R	D [GeV]			
	m_R	$m_R^{(exp.)}$	$\sqrt{s_0}$	pt. model [9]
0^-	1.90 ± 0.03	1.869	2.45 ± 0.15	2.589
1^-	2.00 ± 0.02	2.010	2.55 ± 0.05	2.692
0^+	2.45 ± 0.03	2.351	2.90 ± 0.10	2.949
1^+	2.38 ± 0.05	2.438	2.70 ± 0.10	3.045

$m_{D(1^+)} = 2.38 \pm 0.05$ GeV, which are read off Figs. 4, 5, respectively. Here, we took $\sqrt{s_{D(0^+)}} = 2.8 \sim 3.0$ GeV and $\sqrt{s_{D(1^+)}} = 2.5 \sim 2.8$ GeV, respectively. We summarize these results in Table I. From the table, we find that the excited (p -wave) 1^+ state reproduce the experimental data within errors, while the excited 0^+ state seems to be overestimated by about 100 MeV in comparison with the experimental data. However, if we take into account the broad width ($\Gamma_{D(0^+)} \simeq 329$ MeV) measured by experiments, our result could be not in conflict with such data (within the large width). Also, the obtained thresholds are different among the four channels and thus have a level structure similar to the obtained resonance masses; the order of this energy level is the same as that of the resonance masses.

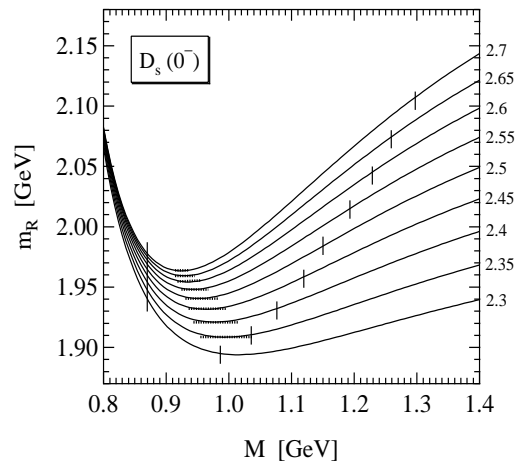


FIG. 6: The Borel curves of $m_{D_s(0^-)}$ vs. M , where $\sqrt{s_{D_s(0^-)}} = 2.3 \sim 2.7$ GeV at 0.05 GeV intervals.

Next, we discuss the case of the $c\bar{s}$ mesons following the above criteria. Here we fix $m_s = 0.12$ GeV as listed before. Indeed, final results of the resonance masses are almost insensitive to the adopted values of m_s . For example, the result with $m_s = 0.15$ GeV changes by less than 0.5% of that with $m_s = 0.12$ GeV. Hence, the error coming from such a mass ambiguity is smaller than the error originated from the criteria mentioned above. We show

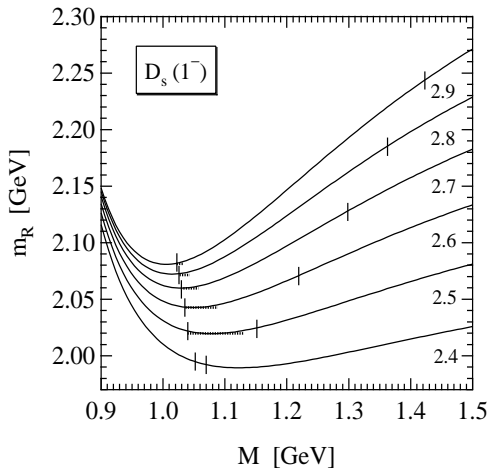


FIG. 7: The Borel curves of $m_{D_s(1^-)}$ vs. M , where $\sqrt{s_{D_s(1^-)}} = 2.4 \sim 2.9$ GeV at 0.1 GeV intervals.

the results of the 0^- channel in Fig. 6. The behaviors of the curves and the Borel windows are very close to those of the $D(0^-)$ in Fig. 2. We get $m_{D_s(0^-)} = 1.94 \pm 0.03$ GeV for $\sqrt{s_{D_s(0^-)}} = 2.3 \sim 2.7$ GeV by applying the above criteria. This value is almost consistent with the experimental data (1.969 GeV) within errors and higher by 40 MeV than our result for the $c\bar{n}$ meson. Thus, our mass-splitting between the $D_s(0^-)$ and $D(0^-)$ is underestimated by about 100 MeV in comparison with the measured one, which would just correspond to a deviation between light-quark and strange-quark masses. Another

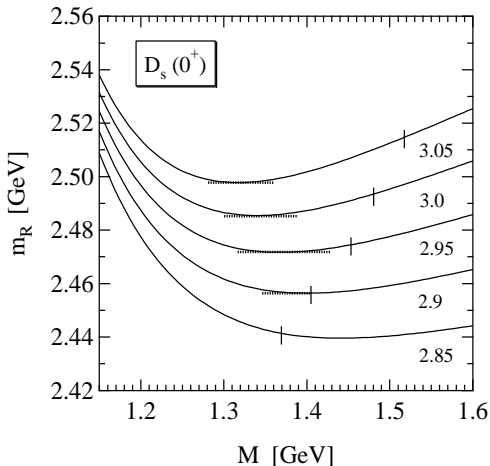


FIG. 8: The Borel curves of $m_{D_s(0^+)}$ vs. M , where $\sqrt{s_{D_s(0^+)}} = 2.85 \sim 3.05$ GeV at 0.05 GeV intervals. The lower limits of the Borel windows are below $M = 1.15$ GeV.

remarkable point is that there exists also a deviation between their thresholds as well as the mass-splitting of the resonance masses. This deviation is near the value of the mass-splitting. It is, therefore, expected that such a deviation for the thresholds plays an essential role to

give the mass-splitting of the resonance masses. We

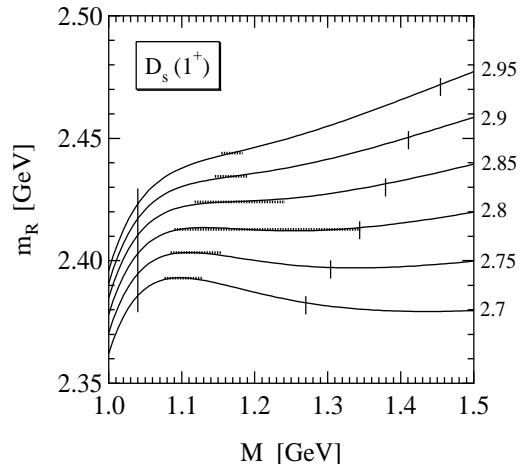


FIG. 9: The Borel curves of $m_{D_s(1^+)}$ vs. M , where $\sqrt{s_{D_s(1^+)}} = 2.7 \sim 2.95$ GeV at 0.05 GeV intervals.

also show numerical results of other three channels in Figs. 7, 8, 9 in the same analysis. Every graph has the curves similar to the corresponding channel of the $c\bar{n}$ meson, respectively. In the 1^- channel, the obtained mass $m_{D_s(1^-)} = 2.05 \pm 0.04$ GeV for $\sqrt{s_{D_s(1^-)}} = 2.4 \sim 2.9$ GeV is somewhat smaller than the experimental data (2.112 GeV) like the case of the $c\bar{n}$ meson. In this channel also, our mass-splitting between the $D_s(1^-)$ and $D(1^-)$ is about a half of the experimental observation, *i.e.* ~ 50 MeV, and also a difference of the obtained thresholds between their mesons is non-zero, *i.e.* about 100 MeV. In the 0^+ channel, we find that the obtained mass $m_{D_s(0^+)} = 2.48 \pm 0.03$ GeV for $\sqrt{s_{D_s(0^+)}} = 2.85 \sim 3.05$ GeV is overestimated by about 160 MeV compared with the experimental data (2.317 GeV), as seen in the case of the $D(0^+)$. This result is very close to that from the potential models [8, 9]. Contrary to the case of the $D(0^+)$, the $D_s(0^+)$ meson has been observed as the very narrow state ($\Gamma_{D_s(0^+)} \leq 4.6$ MeV). Therefore, this deviation (160 MeV) is significant and our result supports conclusions from Ref. [8, 9, 10, 11, 12]. A deviation between the thresholds of the $D_s(0^+)$ and $D(0^+)$ is about 100 MeV. In contradiction to the result in Ref. [8, 9], however, our result in the 1^+ channel, $m_{D_s(1^+)} = 2.41 \pm 0.05$ GeV for $\sqrt{s_{D_s(1^+)}} = 2.7 \sim 2.95$ GeV, is in agreement with the experimental data (2.459 GeV) within errors. Such agreement with the data could be due to disregard of mixing effects between $J^{P(C)} = 1^{+(+)}$ and $1^{+(-)}$, although Refs. [8, 9] have taken into account the effect. Here, our result for the threshold gives almost the same value with the case of $D(1^+)$. These final results for four channels of the $c\bar{s}$ mesons are summarized in Table II.

TABLE II: Numerical results of the resonance mass m_R and the continuum threshold $\sqrt{s_R}$. They are listed for four channels ($R = 0^-, 1^-, 0^+, 1^+$) of the $c\bar{s}$ mesons. For comparison, we attach experimental average values observed recently [2, 3, 4, 5, 6] in each channel and the masses of the first radial excitations, which is predicted in Ref. [9].

R	m_R	D_s [GeV]		pt. model [9]
		$m_R(\text{exp.})$	$\sqrt{s_0}$	
0^-	1.94 ± 0.03	1.969	2.50 ± 0.20	2.700
1^-	2.05 ± 0.04	2.112	2.65 ± 0.15	2.806
0^+	2.48 ± 0.03	2.317	3.00 ± 0.15	3.067
1^+	2.41 ± 0.05	2.459	2.70 ± 0.25	3.165

V. SUMMARY AND DISCUSSION

We have presented detailed calculations of the masses for the $0^-, 1^-, 0^+, 1^+$ charmed-mesons (D, D_s), motivated by recent discovery of very narrow two states ($D_{s0}^{*+}(2317), D_{s1}^{*+}(2459)$) by the BABAR, CLEO, BELLE and FOCUS Collaborations. Applying the original QSR techniques of SVZ [22] for the conventional light-heavy systems, we have performed the OPE up to $d = 6$, involving corrections to the order α_s and to the order m_s (or m_n). In this method we have taken into account full order of the $1/m_c$ -expansion, because m_c is not a large mass enough to approximate by the first few terms of the expansion. We have analyzed their masses using the Borel-transformed QSR, because this analysis can carefully deal with the continuum contribution or the threshold dependence, if the resonance mass, which we would derive from this analysis, is sensitive to such a contribution [46]. Especially, such care is important for discussion of the spectroscopy associated with (hyper-)fine structures as in our considering four channels. In fact, as seen in Tables I and II, we found that the mass-splittings among four channels of the $c\bar{n}$ or $c\bar{s}$ mesons and those in the same channels between the $c\bar{n}$ and $c\bar{s}$ mesons can be largely affected by the values of their thresholds. In order to derive a reliable resonance mass from the threshold dependence, we performed numerical calculations by imposing stringent criteria listed in sec. IV for the BSR. We compare our final results for resonance masses of $c\bar{n}$ and $c\bar{s}$ mesons with those of the experimental data in Fig. 10. From this figure, we find that the mass of the $D_s(0^+)$ meson is overestimated by about 160 MeV in comparison with the experimental data, which is consistent with the potential model analysis [8, 9]. Although a similar tendency is also seen in the mass of the $c\bar{n}$ meson in the same channel, these results could be consistent with the experimental data within the measured broad width. On the other hand, such a tendency is not seen in other channels. Conversely in other channels the $c\bar{s}$ masses are underestimated somewhat in comparison with data, independent of strange-quark mass adopted in our calculations. Hence, the $1^+ - 1^-$ and the $0^+ - 0^-$ mass-splittings are unequal in disagreement with the chiral multiplet

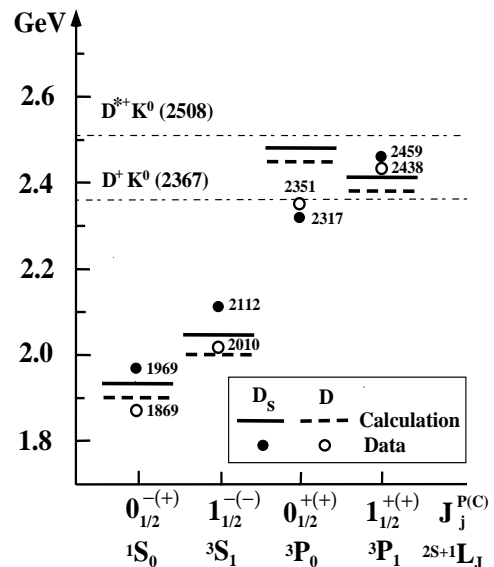


FIG. 10: Spectroscopy of the $c\bar{n}$ and $c\bar{s}$ mesons with $J^P = 0^-, 1^-, 0^+, 1^+$. The solid lines for the $c\bar{s}$ mesons and dashed lines for the $c\bar{n}$ mesons show our numerical results. The corresponding experimental data are given by closed and open circles, respectively, as in Fig. 1.

structure predicted by chiral effective theory for heavy mesons. It might be expected that the measured low mass of $D_s^{*+}(2317)$ is a manifestation of any exotic states with the structure of a four-quarks or a molecule. In fact, we have seen very recently [29] that the assignment of the $D_{s0}^{*+}(2317)$ to the charmed-strange four-quark meson, \hat{F}_1 , with $(I, I_3) = (1, 0)$ is favored by the ratio of the measured rates for the $D_{s0}^{*+}(2317) \rightarrow D_s^{*+}\gamma$ to the $D_{s0}^{*+}(2317) \rightarrow D_s^+\pi^0$ decay [4], $\Gamma(D_s^{*+}\gamma)/\Gamma(D_s^+\pi^0) < 0.052$. It is, however, hard to reconcile its assignment to an isosinglet state (the conventional $\{c\bar{s}\}$ or an isosinglet four-quark or a molecule) with the experimental constraint. Our conclusion for the charmed mesons with 0^+ is different from that of Ref. [23], where the similar QSR analysis was performed only for 0^- and 0^+ states of the $c\bar{s}$ and $c\bar{n}$ -mesons without using stringent criteria like in our analysis.

In this work, we neglected renormalization-group improvement for the currents and the operators in the condensates, which could be important to improve the Q^2 range of the validity of the derived QSR. Also, as is well known, the physical quantities extracted from the QSR analysis generally have theoretical ambiguity of about $10 \sim 20\%$, which comes from the condensates and our criteria, *etc.* However, these quantitative ambiguities would not qualitatively change our conclusion as mentioned above, because we have evaluated totally eight states of the $c\bar{n}$ and $c\bar{s}$ mesons within the same method and criteria. In such an analysis we found an anomalous feature for only the charmed-strange scalar meson.

Acknowledgments

We are grateful to S. Sasaki for fruitful discussion and M. Harada for a useful comment. The research of A.H. is supported by the research fellowship from Department

of Physics, Kyoto University. This work of K.T. is supported in part by the Grant-in-Aid for Science Research, Ministry of Education, Science and Culture, Japan (No. 13135101 and No. 16540243).

-
- [1] S. Godfrey and N. Isgur, Phys. Rev. **D32**, 189 (1985).
 [2] BABAR Collaboration, B. Aubert *et al.*, Phys. Rev. Lett. **90**, 242001 (2003).
 [3] BABAR Collaboration, B. Aubert *et al.*, Phys. Rev. **D69**, 031101 (2004).
 [4] CLEO Collaboration, D. Besson *et al.*, Phys. Rev. **D68**, 032002 (2003).
 [5] BELLE Collaboration, K. Abe *et al.*, Phys. Rev. **D69**, 112002 (2004).
 [6] FOCUS Collaboration, E.W. Vaandering, hep-ex/0406044.
 [7] J. Bartelt and S. Shukla, Ann. Rev. Nucl. Part. Sci. **45**, 133 (1995) and references therein.
 [8] S. Godfrey and R. Kokoski, Phys. Rev. **D43**, 1679 (1991).
 [9] M. Di Pierro and E. Eichten, Phys. Rev. **D64**, 114004 (2001).
 [10] R.N. Cahn and J.D. Jackson, Phys. Rev. **D68**, 037502 (2003).
 [11] Y.-B. Dai, C.-S. Huang, C. Liu and S.-L. Zhu, Phys. Rev. **D68**, 114011 (2003).
 [12] G.S. Bali, Phys. Rev. **D68**, 071501(R) (2003).
 [13] A. Dougall, R.D. Kenway, C.M. Maynard and C. McNeile, the UKQCD Collaboration, Phys. Lett. **B569**, 41 (2003).
 [14] M.A. Nowak, M. Rho and I. Zahed, Phys. Rev. **D48**, 4370 (1993); W.A. Bardeen and C.T. Hill, Phys. Rev. **D49**, 409 (1994).
 [15] W.A. Bardeen, E.J. Eichten and C.T. Hill, Phys. Rev. **D68**, 054024 (2003).
 [16] E. van Beveren and G. Rupp, Phys. Rev. Lett. **91**, 012003 (2003).
 [17] T. Barnes, F.E. Close and H.J. Lipkin, Phys. Rev. **D68**, 054006 (2003).
 [18] A.P. Szczepaniak, Phys. Lett. **B567**, 23 (2003).
 [19] H.-Y. Cheng and W.-S. Hou, Phys. Lett. **B566**, 193 (2003).
 [20] K. Terasaki, Phys. Rev. **D68**, 011501(R) (2003); hep-ph/0309119; hep-ph/0309279; hep-ph/0311069; hep-ph/0405146.
 [21] T. Browder, S. Pakvasa and A.A. Petrov, Phys. Lett. **B578**, 365 (2004).
 [22] M.A. Shifman, A.I. Vainstein and V.I. Zakharov, Nucl. Phys. **B147**, 385, 448 (1979).
 [23] S. Narison, hep-ph/0307248.
 [24] Particle Data Group Collaboration, S. Eidelman *et al.*, Phys. Lett. **B592**, 1 (2004).
 [25] CLEO Collaboration, S. Anderson *et al.*, Nucl. Phys. **A663**, 647 (2000).
 [26] BELLE Collaboration, P. Krokovny *et al.*, Phys. Rev. Lett. **91**, 262002 (2003).
 [27] FOCUS Collaboration, J.M. Link *et al.*, Phys. Lett. **B586**, 11 (2004).
 [28] Indeed, the study for the 1^+ state would be more complicated than that for the 0^+ state. It is, *e.g.*, because two states such as $J^{P(C)} = 1^{+(+)}, 1^{+(-)}$ can take place a mixing between them as mentioned in the text above.
 [29] A. Hayashigaki and K. Terasaki, hep-ph/0410393.
 [30] C.-H. Chen and H.-n. Li, Phys. Rev. **D69**, 054002 (2004).
 [31] H.J. Lipkin, Phys. Lett. **B580**, 50 (2004).
 [32] L.J. Rindeers, H.R. Rubinstein and S. Yazaki, Phys. Rep. **127**, 1 (1985).
 [33] T. Hatsuda, Y. Koike and S.H. Lee, Nucl. Phys. **B394**, 221 (1993).
 [34] V.A. Novikov, M.A. Shifman, A.I. Vainstein and V.I. Zakharov, Fortschr. Phys. **32**, 11, 585 (1984).
 [35] L.J. Reinders, H.R. Rubinstein and S. Yazaki, Phys. Lett. **97B**, 257 (1980).
 [36] S. Narison, "QCD as a Theory of Hadrons, From Partons to Confinement", Cambridge University Press (2004) and references therein.
 [37] L.J. Reinders, S. Yazaki and H.R. Rubinstein, Phys. Lett. **103B**, 63 (1981).
 [38] The value of α_s at any scale can be obtained from <http://www-theory.lbl.gov/~ianh/alpha/alpha.html>.
 [39] T. Hatsuda, Y. Koike and S.H. Lee, Phys. Rev. **C47**, 1225 (1993); The final analytic forms of the BSR in this paper have two trivial typos: first, the sign of the term with dimension-4 operators in the axial-vector channel should be minus and second, the factor of α_s correction in the scalar channel should be 9/3.
 [40] T.M. Aliev and V.L. Eletsy, Sov. J. Nucl. Phys. **38**(6), 936 (1984).
 [41] V.L. Eletsy, Phys. Atom. Nucl. **59**, 2002 (1996).
 [42] This value is very close to a pole mass used in Ref. [23, 45].
 [43] X. Jin, T.D. Cohen, R.J. Furnstahl and D.K. Griegel, Phys. Rev. **C47**, 2882 (1993).
 [44] L.J. Reinders, H.R. Rubinstein and S. Yazaki, Nucl. Phys. **B186**, 109 (1981).
 [45] S. Narison, Phys. Lett. **B520**, 115 (2001)
 [46] We also checked the resonance masses by using finite energy sum rule. However, this method shows strong dependence of their masses on the continuum thresholds and we cannot get reliable masses with enough accuracy like the BSR.